AIAA JOURNAL
Vol. 32, No. 4, April 1994

Role of Kutta Waves on Oscillatory Shock Motion on an Airfoil

B. H. K. Lee* and H. Murty†
National Research Council, Ottawa, Ontario, Canada
and
H. Jiang‡
Queen's University, Kingston, Ontario, Canada

An investigation of wave propagation in transonic flows is carried out using the nonlinear transonic small disturbance equation. The wave fronts are computed from numerical integration of the characteristic equation. The manner in which downstream disturbances, initiated at an airfoil trailing edge, travel to the shock wave is analyzed. Though a relation between the amplitude of the disturbance and the magnitude of shock displacement has not yet been derived to study the interaction process, the results presented are sufficient to give a better understanding of the feedback mechanism proposed in an earlier investigation of oscillatory shock motion observed in transonic airfoil buffeting. The propagation time for downstream disturbances to reach the shock wave is computed for various airfoil geometries and freestream Mach numbers. The results are compared with those obtained from an empirical formulation given by Tijdeman. The accuracy of Tijdeman's relaxation factor is examined. The interaction of upstream moving waves with a time-dependent flowfield is also studied for an airfoil performing trailing-edge flap oscillations. The variation of the disturbance amplitude along the wave front at various instances of time is given for an impulse source at the trailing edge using the method of asymptotic expansion.

Nomenclature

A = coefficient in transonic small disturbance equation
a_n = coefficients of asymptotic expansion
a_1 = wave amplitude
B = coefficient in transonic small disturbance equation
C = coefficient in transonic small disturbance equation
c = chord
c_{gr} = group velocity
c_{ph} = phase velocity
F = Eikonal function
H = characteristic function
M_∞ = freestream Mach number
(p, q) = normal of wave fronts
R = Tijdeman's empirical constant
S = phase function
T = time normalized with respect to c/U_∞
T_p = propagation time
t = time scaled by ω^{-1}, deg
U_∞ = freestream velocity
x_s = shock wave location
(x, y) = Cartesian coordinates normalized with respect to c
α = initial angle of wave front normal
α_{cr} = critical initial angle, deg
α_I = ray angle giving closest agreement between numerical and Tijdeman's results
θ = phase
κ = reduced frequency $\omega c/U_\infty$
(ξ, η) = wave numbers
Φ = total potential, $\phi + \psi$
ϕ = potential in transonic small disturbance equation
ψ = disturbance potential
Ω = frequency function
ω = frequency

Received March 1, 1993; presented as Paper 93-1589 at the AIAA/ASME/ASCE/AHS/ASC 34th Structures, Structural Dynamics, and Materials Conference, La Jolla, CA, April 19–21, 1993; revision received Oct. 4, 1993; accepted for publication Oct. 18, 1993.

*Senior Research Officer, High Speed Aerodynamics Laboratory, Institute for Aerospace Research; also Adjunct Professor, Department of Mechanical Engineering, University of Ottawa, Ottawa, Ontario, Canada. Associate Fellow AIAA.

†Guest Worker, Department of Mechanical Engineering, University of Ottawa, Ottawa, Ontario, Canada. Member AIAA.

‡Assistant Professor, Department of Computing and Information Science.

Introduction

PERIODIC shock motions on airfoils in transonic flows have been observed experimentally by various authors.[1–6] Spark schlieren photographs of flowfields indicate clearly the presence of upstream moving waves originating at the trailing edge and near-wake region. They are associated with wake fluctuations due to unsteady shock motions and termed "Kutta waves" by Tijdeman.[1]

Several explanations of the mechanisms of shock wave oscillations have been advanced by various authors[3–6] in their interpretation of experimental results performed with different airfoils and flow conditions. Mundell and Mabey[3] investigated transonic wind-tunnel wall interference. They suggested that when the shock wave from the airfoil meets the boundary layer on the roof of the wind tunnel, disturbances can propagate upstream along the subsonic portion of the boundary layer and feed back through the freestream to cause shock oscillations. For symmetric airfoils at zero incidence, such as the 14% Biconvex and NACA 0012 airfoils, Gibb[4] postulated that disturbances on one surface will cause an upward deflection of the wake similar to the deflection of a trailing-edge flap. The asymmetric wake causes the shock on the other surface to move toward the rear. The shock waves move in antiphase, and the wake is displaced toward the surface on which the separation is taking place. Antiphase motions of the shock waves are required to generate self-sustained shock oscillations. Stanewsky and Basler[5] performed a wind-tunnel investigation of the buffet characteristics of the CAST 7/DOA1 airfoil. They proposed that the thickening of the boundary layer at the trailing edge and the

corresponding drop in trailing-edge pressure drive the shock upstream since the shock strength must adjust according to the trailing-edge pressure. The thickening of the boundary layer at the trailing edge also causes a decambering of the airfoil. This reduces the circulation and results in a decrease of the supersonic region and hence the shock strength. Pressure disturbances generated must travel via the lower surface where the flow is being accelerated due to the pressure drop at the trailing edge. On reaching the leading-edge region, these waves cause a change in the stagnation point location. A new flowfield is developed on the upper surface, and the feedback mechanism for self-sustained shock motion is primarily through the boundary layer.

In Ref. 6, a model to predict the unsteady shock motion observed in buffeting flows was formulated. An explanation of the mechanism of self-sustained shock oscillation and a method to estimate the frequency of oscillation were given. The case of a shock wave oscillating on the upper airfoil surface about a mean position was considered (corresponding to Tijdeman's[1] type A shock motion). The model assumed that the flow behind the shock boundary-layer interaction to be fully separated. Pressure waves, formed as a result of the movement of the shock, propagate downstream in the separated flow region. On reaching the trailing edge, the disturbances generate upstream moving waves as a result of satisfying the unsteady "Kutta" condition. The upstream moving waves, termed Kutta waves, interact with the shock and impart energy to return it to its initial location. The loop is then completed. The period of shock wave oscillation is found by Lee[6] to agree with the time it takes for a disturbance to propagate from the shock to the trailing edge plus the duration for an upstream wave to reach the shock from the trailing edge.

Detailed measurements of the pressure disturbance velocities for various flow conditions on the Bauer-Garabedian-Korn no. 1 supercritical airfoil have been carried out in Ref. 7. The upstream moving wave velocities outside the separated flow region could not be easily measured experimentally but were estimated using an empirical formula given by Tijdeman[1] based on the measured steady surface Mach number along the airfoil. The shock wave can be affected by upstream moving disturbances that propagate in the thin separated flow on the airfoil surface. However, in the analysis given in Ref. 6, the upstream moving waves in the inviscid flowfield outside the separated flow region carry the bulk of the energy to the shock to maintain its oscillatory motion. Disturbances can originate in the separated flow region on the airfoil, but they are weak compared with those generated at the trailing edge and hence are neglected by Lee.[6]

The use of an empirical constant in Tijdeman's equation has raised some questions as to the universality of the constant for different airfoils. To assess the accuracy of the use of Tijdeman's expression for the Kutta waves, we analyzed the propagation of wave fronts in transonic flows in this paper using the nonlinear transonic small disturbance equation. The effects of Mach number and airfoil thickness are investigated, and the results are compared with those using Tijdeman's empirical formulation.

Earlier study of wave propagation in transonic flows has been carried out by Spee.[8] The study was mainly concerned with the stability of smooth transonic flows past airfoils and the generation of shock waves in transonic two-dimensional flows. The construction of the wave pattern is based on the principle that the propagation velocity normal to the wave fronts is equal to the local speed of sound. The procedure used was not described in any detail in Spee's report, but it is presumed that a numerical/graphical construction method was used. Spee[8] noted that the accuracy of the constructed wave pattern is only good enough to draw rough conclusions on the manner in which waves propagate in transonic flows. However, the analysis demonstrates clearly how disturbances can travel through the supersonic region.

Wave propagation in an unsteady flowfield is of interest in aeroelastic applications. The airfoil may be performing pitch or plunge motions. Also, the trailing-edge flap may be oscillating. Since the flowfield is time dependent, a disturbance wave front at any point in space and time depends on the flow conditions when the initial waveform is generated. Some studies on the interaction of Kutta waves with an unsteady flowfield generated by an airfoil performing trailing-edge flap oscillations are carried out. The results are useful in the study of wave propagation on an elastic wing performing oscillatory motion. Only preliminary results of a pulse propagating in a time-dependent medium are shown in this paper. The more complicated case of the interaction of a harmonic disturbance with a shock wave having different frequencies of oscillations will be presented in a later paper. The relation between the amplitude of the disturbance and the magnitude of shock motion will also be addressed in that paper.

Analysis

Characteristic Surface

To investigate the propagation of pressure disturbances in transonic flows, we used the method of characteristics. The time variation of the characteristic surfaces describes the propagation of discontinuities in the flowfield.

The formulation is based on the nonconservative form of the nonlinear transonic small disturbance equation

$$A\phi_{tt} + 2B\phi_{xt} = C\phi_{xx} + \phi_{yy} \tag{1}$$

where

$$A = M_\infty^2\kappa^2, \quad B = M_\infty^2\kappa, \quad C = (1 - M_\infty^2) - (\gamma + 1)M_\infty^2\phi_x \tag{2}$$

To find a characteristic surface for Eq. (1), it is assumed that the potential ϕ and its gradient $\nabla\phi$ are continuous, but the second derivatives of ϕ have jump discontinuities across a surface described by $H(x, y, t) = \text{const}$. Thus, on the surface of a discontinuity, the function H satisfies the equation

$$H_t^2 + 2A^{-1}BH_xH_t - A^{-1}CH_x^2 - A^{-1}H_y^2 = 0 \tag{3}$$

This equation is referred to as the characteristic equation of Eq. (1), and a solution of Eq. (3) defines a characteristic surface $H = \text{const}$.

The characteristic surface $H = \text{const}$ can also be described by the following equation:

$$H(t, x, y) \equiv t - S(x, y) = 0 \quad \text{or} \quad t = S(x, y) \tag{4}$$

The substitution of $H = t - S$ into Eq. (3) yields the following equation for $S(x, y)$:

$$1 - 2A^{-1}BS_x - A^{-1}CS_x^2 - A^{-1}S_y^2 = 0$$

Introducing the variables $p = S_x$ and $q = S_y$, and adding and subtracting a term $(A^{-1}B)^2p^2$, the previous equation becomes

$$F(x, y, S, p, q) \equiv -1 + A^{-1}Bp + A^{-1}\sqrt{(B^2 + AC)p^2 + Aq^2} = 0 \tag{5}$$

On the characteristic surface, $t = S$, $\phi = \phi(S, x, y)$, and therefore C in Eq. (2) is a function of x, y, S. Equation (5) is often called the Eikonal equation,[9] and a solution for S can

be obtained parametrically by a system of ordinary differential equations[10]:

$$\begin{aligned}\frac{dx}{dt} &= A^{-1}B + \frac{(B^2 + AC)p}{A\sqrt{(B^2 + AC)p^2 + Aq^2}}\\ \frac{dy}{dt} &= \frac{q}{\sqrt{(B^2 + AC)p^2 + Aq^2}}\\ \frac{dp}{dt} &= \frac{-C_x p^2 - C_t p^3}{2\sqrt{(B^2 + AC)p^2 + Aq^2}}\\ \frac{dq}{dt} &= \frac{-C_y p^2 - C_t p^2 q}{2\sqrt{(B^2 + AC)p^2 + Aq^2}}\end{aligned} \tag{6}$$

where

$$C_x = -(\gamma + 1)M_\infty^2\phi_{xx}, \qquad C_y = -(\gamma + 1)M_\infty^2\phi_{xy}$$
$$C_t = -(\gamma + 1)M_\infty^2\phi_{xt} \tag{7}$$

This system of equations describes how disturbances in the form of discontinuities propagate in the unsteady transonic flowfield. Once a particular solution ϕ is known, Eqs. (6) can be used to compute the wave propagation in transonic flows.

Figure 1 shows a schematic of the wave fronts generated above the upper surface of an airfoil from a source placed at the trailing edge. The equation $S(x, y) = t$ describes a wave front at a given time t. Thus $(p, q) = (S_x, S_y)$ is parallel to the normal to the wave fronts. The vector $(dx/dt, dy/dt)$ is the direction of rays. A ray is an integral curve $[x(t), y(t)]$ of Eq. (6) that defines the path followed by a disturbance to reach its destination. As was shown in Ref. 11, the first two equations in Eqs. (6) give the group velocity $(\dot{x}, \dot{y})$. It is difficult to integrate Eqs. (6) analytically, but they can be solved numerically to obtain the speed of propagation of the characteristic surface at any given time and location.

Initial Conditions

The trajectory $[x(t), y(t)]$, $t > t_0$, is a ray starting at the initial position (x_0, y_0). For homogeneous and isotropic flows, the rays are parallel to the normal directions; that is, they are orthogonal to the wave fronts. In the general case, however, the rays are not parallel to the normal directions, which implies that the wave fronts may not be propagated along the rays.

In the study of upstream wave propagation, considerable simplification in the analysis can be obtained by assuming the initial disturbance to be represented by an impulse function

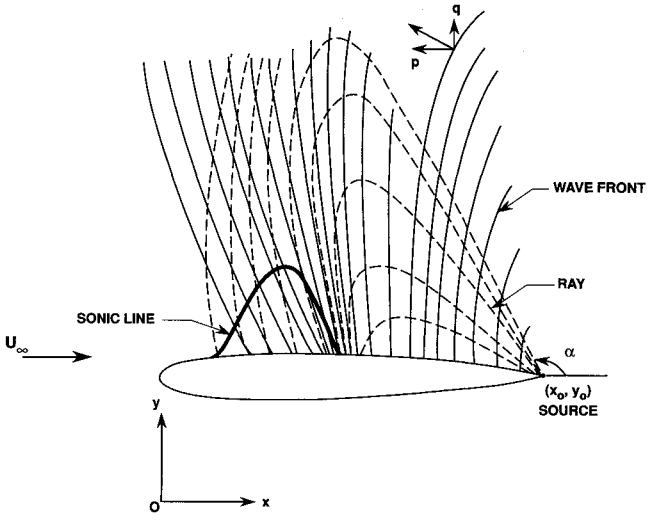

Fig. 1 Schematic of wave fronts and rays emanating from source disturbance at trailing edge of airfoil.

at a point (x_0, y_0). At time $t = t_0$, the wave front due to the impulse may be thought of as a circle of infinitesimal radius. In other words, each point on the initial wave front has the same position (x_0, y_0), but the normal direction is given by

$$(p_0, q_0) = [r\cos(\alpha), r\sin(\alpha)], \qquad 0 \le \alpha \le 2\pi \tag{8}$$

The radius r is determined by requiring the initial wave front to be on a characteristic surface. When Eq. (8) is substituted into Eq. (5), r can be obtained in terms of α, as well as x_0, y_0. For a given $\alpha \in (0, 2\pi)$, Eq. (6) can be integrated in time to yield the solution

$$x = x(t, \alpha), \quad y = y(t, \alpha), \quad p = p(t, \alpha), \quad q = q(t, \alpha) \tag{9}$$

Equation (9) describes the propagation of a pulse disturbance that is initiated at the time t_0 from the point source at (x_0, y_0). For a fixed angle α, $[x(t, \alpha), y(t, \alpha)]$, $t > t_0$, is the ray of propagation of the energy. For a fixed time $t > t_0$, $[x(t, \alpha), y(t, \alpha)]$, $0 < \alpha < 2\pi$, describes the wave front of the pulse disturbances at the time t.

Asymptotic Expansion

In this section, the propagation of disturbances from a point source in a time-dependent flowfield around an oscillating airfoil is considered. The method of asymptotic expansion is a convenient technique for obtaining an approximate solution to the propagation of a point source disturbance in a time-dependent medium. In this approach, the unsteady medium is computed from the solution of the transonic flow around an oscillating airfoil. There are a number of computer codes developed for unsteady airfoil motions. In this paper, the code developed by Couston and Angelini[12] is used.

Representing the total flow potential Φ by the sum

$$\Phi = \phi + \psi \tag{10}$$

where ϕ is due to the unsteady oscillation of the airfoil, and ψ is due to the disturbance source. An equation for ψ can be found if Eq. (10) is substituted into Eq. (1). Since ϕ satisfies Eq. (1), an equation for ψ can be found to be

$$A\psi_{tt} + 2B\psi_{xt} = C\psi_{xx} + \psi_{yy} + D(\psi_x\psi_{xx} + \phi_{xx}\psi_x) \tag{11}$$

where A, B, and C are defined by Eq. (2) and $D = -(\gamma + 1)M_\infty^2$.

Assuming that the amplitude of the disturbance generated by the source is of a higher order than the perturbed flowfield around the oscillating airfoil, ψ can be expressed by the following,

$$\psi = e^{i\theta}\sum_{n=1}\varepsilon^n a_n(t, x, y) \tag{12}$$

where $\theta = \theta(t, x, y)$, and $a_n(t, x, y)$ are slowly varying functions. Furthermore, the term ϕ_x is also assumed to be slowly varying. More precisely, θ_t, θ_x, θ_y, $\phi_x = \mathcal{O}(1)$, and a_{nt}, a_{nx}, a_{ny}, $\phi_{xx} = \mathcal{O}(\varepsilon)$. Each additional derivative increases the order by ε. Following Whitham,[9] the following substitutions are made:

$$\begin{aligned}\theta(t, x, y) &= \varepsilon^{-1}\tilde{\theta}(\varepsilon t, \varepsilon x, \varepsilon y)\\ a_n(t, x, y) &= \tilde{a}_n(\varepsilon t, \varepsilon x, \varepsilon y)\\ \phi_x(t, x, y) &= \tilde{\phi}_x(\varepsilon t, \varepsilon x, \varepsilon y)\end{aligned} \tag{13}$$

where $\tilde{\theta}$, $\tilde{a}_n$, $\tilde{\phi}_x$, and their derivatives are all $\mathcal{O}(1)$.

Define the wave numbers and the frequency by

$$\omega = \theta_t, \qquad \xi = -\theta_x, \qquad \eta = -\theta_y \tag{14}$$

When Eqs. (13) and (12) are substituted into Eq. (11), and after dropping the ˜ notation, the ε order equation gives rise to

$$A\omega^2 - 2B\omega\xi - C\xi^2 - \eta^2 = 0 \tag{15}$$

The ε^2 order equation yields a relation for a_1, which leads to the following equation after averaging over one period of θ,

$$\frac{\partial}{\partial t}[(A\omega - B\xi)a_1^2] + \frac{\partial}{\partial x}[(B\omega + C\xi)a_1^2] + \frac{\partial}{\partial y}(\eta a_1^2) = 0 \tag{16}$$

Finally, since $\omega = \theta_t$, $\xi = -\theta_x$, and $\eta = -\theta_y$, the following equations of consistency are obtained:

$$\frac{\partial\omega}{\partial x} + \frac{\partial\xi}{\partial t} = 0, \qquad \frac{\partial\omega}{\partial y} + \frac{\partial\eta}{\partial t} = 0, \qquad \frac{\partial\xi}{\partial y} - \frac{\partial\eta}{\partial x} = 0 \tag{17}$$

Equations (15–17) describe the refraction of frequency and wave numbers and the propagation of wave energy. Solving for ω in Eq. (15), the expression for ω becomes

$$\omega = \Omega(x, y, t, \xi, \eta) \equiv A^{-1}B\xi + A^{-1}\sqrt{(B^2 + AC)\xi^2 + A\eta^2} \tag{18}$$

Equation (18) together with Eq. (17) leads to a system of equations for (x, y, ξ, η). It can be shown that this system of equations is equivalent to Eq. (6) if the following substitution is made:

$$p = \frac{\xi}{\omega}, \qquad q = \frac{\eta}{\omega} \tag{19}$$

Therefore, Eq. (6) not only describes the propagation of the characteristic surfaces but also describes the propagation of the wave solution of Eq. (12).

The first two equations in Eq. (6) define rays or bicharacteristic curves. Along the rays, wave numbers propagate according to the third and fourth equations in Eqs. (6). For a homogeneous medium, the right-hand sides in the third and fourth equations of Eqs. (6) are zero, so that the wave numbers are constant along a ray. Waves of the same wavelengths can be found along a ray. In the general case, however, the wave numbers are not constant, and there are refractions of wave numbers along the rays.

Wave Amplitude

The wave amplitude can be computed by solving Eq. (16) where the quantity a_1 is the amplitude of the leading term in the expansion of ψ. Using Eqs. (15) and (17), Eq. (16) becomes

$$\frac{\partial a_1^2}{\partial t} + \frac{\partial}{\partial x}(\Omega_\xi a_1^2) + \frac{\partial}{\partial y}(\Omega_\eta a_1^2) = 0 \tag{20}$$

where $(\Omega_\xi, \Omega_\eta)$ is the group velocity whose components are given by the following:

$$\Omega_\xi = A^{-1}B + \frac{(B^2 + AC)\xi}{A\sqrt{(B^2 + AC)\xi^2 + A\eta^2}}$$

$$\Omega_\eta = \frac{\eta}{\sqrt{(B^2 + AC)\xi^2 + A\eta^2}}$$

Equation (20) is in the form of a conservation law. To calculate a_1, a wave volume V bounded by rays is considered. The wave volume propagates at the group velocity along the space-time rays. Integrating both sides of Eq. (20) over the volume V results in the following equation:

$$\iiint_V \left[\frac{\partial a_1^2}{\partial t} + \frac{\partial}{\partial x}(\Omega_\xi a_1^2) + \frac{\partial}{\partial y}(\Omega_\eta a_1^2)\right] dV = 0 \tag{21}$$

The divergence theorem gives

$$\iint_S \boldsymbol{n}\cdot(1, \Omega_\xi, \Omega_\eta)^t a_1^2\, dS = 0 \tag{22}$$

where $\boldsymbol{n}$ is the outward normal of the boundary surface S, and the surface integral is over the sides Σ and the ends S_1 and S_2. Since the surface Σ is formed by rays, $\boldsymbol{n}$ is orthogonal to the ray direction $(1, \Omega_\xi, \Omega_\eta)^t$. This implies $\boldsymbol{n}\cdot(1, \Omega_\xi, \Omega_\eta)^t = 0$. On the two ends of V, the normal direction is parallel to the t-axis; therefore $\boldsymbol{n} = (1, 0, 0)^t$ and $\boldsymbol{n}\cdot(1, \Omega_\xi, \Omega_\eta)^t = 1$ on S_2, and $\boldsymbol{n}\cdot(1, \Omega_\xi, \Omega_\eta)^t = -1$ on S_1. Finally, Eq. (22) becomes

$$\iint_{S_1} a_1^2\, dS = \iint_{S_2} a_1^2\, dS \tag{23}$$

The area element S can be chosen to be the area bounded by two rays and two wave fronts. Both the rays originate from the same point source. The rays and wave fronts from a point source disturbance can be parameterized by t and an initial angle α. A ray can be described by $[x(t, \alpha), y(t, \alpha)]$ with α fixed, whereas a wave front is obtained by varying α with t fixed. Thus the area under consideration can be described by

$$\{[x(t, \alpha), y(t, \alpha)] | t_1 \le t \le t_1 + dt,\ \alpha_1 \le \alpha \le \alpha_1 + d\alpha\} \tag{24}$$

The area element can then be calculated by using the Jacobian of the transform $x = x(t, \alpha)$, $y = y(t, \alpha)$, and S can be written as

$$dS = dx\, dy = \left|\frac{\partial(x, y)}{\partial(t, \alpha)}\right| dt\, d\alpha = \frac{D(x, y)}{D(t, \alpha)} dt\, d\alpha \tag{25}$$

Equation (23) can now be written as

$$\iint_{S_1} a_1^2 \frac{D(x, y)}{D(t, \alpha)} dt\, d\alpha = \iint_{S_2} a_1^2 \frac{D(x, y)}{D(t, \alpha)} dt\, d\alpha \tag{26}$$

In the limit as the area approaches 0, Eq. (26) becomes

$$a_1^2 \frac{D(x, y)}{D(t, \alpha)}\bigg|_{t=t_1} = a_1^2 \frac{D(x, y)}{D(t, \alpha)}\bigg|_{t=t_2}$$

or, along a ray,

$$a_1^2 \frac{D(x, y)}{D(t, \alpha)} = \text{const} \tag{27}$$

The amplitude a_1 can be found by calculating

$$\frac{D(x, y)}{D(t, \alpha)} = |x_t y_\alpha - y_t x_\alpha| \tag{28}$$

Equation (28) can be integrated together with the ray equations in Eqs. (6).

Results and Discussion

Propagation of Wave Fronts

To investigate the nature of wave propagation, generated by a disturbance source situated on an airfoil surface, Eqs. (6) are integrated in time using the first-order Euler time-stepping scheme. At each time step, the solution (x, y) from

the first two equations of Eqs. (6) traces out the rays. Using a range of initial angles from $\pi/2$ to π, we can compute wave fronts (x, y) on the airfoil upper surface. The procedure of starting the numerical integration of the ray equations is described in the section on initial conditions.

The behavior of the disturbances depends on the flowfield around the airfoil. The presence of supersonic flow regions and shock waves is important in wave propagation. Crowding or steepening of the wave fronts is observed near the shock wave. In this paper, the positions of rays and wave fronts are shown for the case of a NACA 64A006 airfoil. Other airfoils have been considered at various freestream Mach numbers, and they are found to have a similar influence on the propagation of disturbances.

An example of upstream wave propagation at different times after a disturbance is generated by an impulse source at the airfoil trailing edge is shown in Fig. 2. The freestream Mach number M_∞ is 0.85. The range of initial ray angles $\alpha \in (107, 174$ deg), and the time interval Δt is approximately 0.4 deg, where time is scaled by ω^{-1}. The nonuniformity of the flowfield causes the curvature of the rays to bend toward the surface where the change in velocity is the greatest. At this Mach number, a shock wave is formed at approximately midchord. The Mach number on the airfoil surface upstream of the shock is 1.07. The presence of this shock wave and an associated supersonic pocket increases the curvature of the rays and wave fronts. The pressure change due to disturbances that have traveled upstream of the shock will result in a perturbation to the shock location. The interaction of a finite amplitude disturbance with the shock wave and the resulting amplitude of shock motion cannot be determined from the present analysis. The relation between disturbance amplitude and the magnitude of shock displacement will be presented in a subsequent paper.

For a small increase in M_∞ by 0.01 to 0.86, the surface Mach number upstream of the shock is 1.1, and the shock wave is located close to 0.6 chord. For this slightly stronger supercritical flowfield, significant increase in the curvature of the rays toward the shock wave is observed.[11]

The freestream Mach number is increased further to 0.88, and the subsequent wave fronts and rays are shown in Fig. 3. The supercritical region extends to 0.7 chord in the vertical direction, with a terminating shock wave having an upstream Mach number of 1.18. It is difficult to determine the rays that negotiate upstream beyond the supercritical region. The rays are pushed closer together at the shock because of the large velocity gradient in the strong supersonic flowfield.

The energy of the wave propagates along the rays with the group velocity c_{gr}, whereas the wave fronts travel in the normal direction with the phase velocity c_{ph}. In general, $c_{gr} \neq c_{ph}$. This is quite evident in the local supersonic region where the energy propagates downstream but the wave fronts move upstream. A wave front in this region bends in such a way that its normal vector c_{ph} has a positive component in the upstream direction. It was shown in Ref. 11 that on projection of c_{gr} on the wave normal its magnitude is equal to c_{ph}.

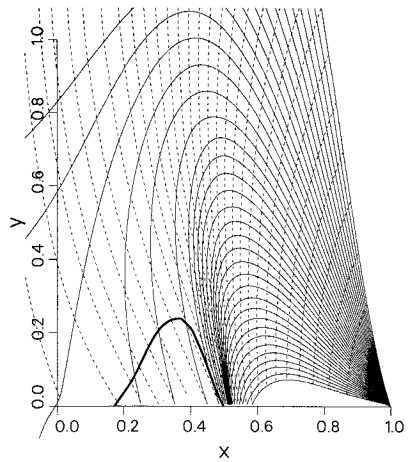

Fig. 2 Wave fronts and rays on the upper surface of a NACA 64A006 airfoil at M_∞ = 0.85 generated by an impulse source at the trailing edge: -----, wave front; ——, ray; ———, sonic line.

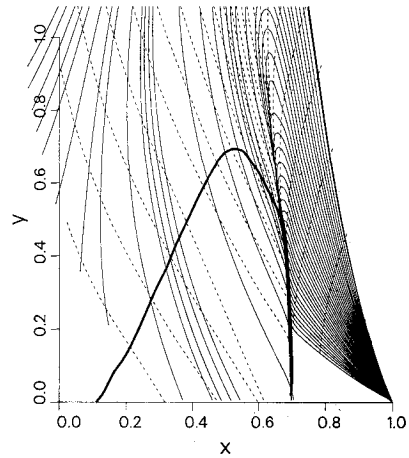

Fig. 3 Wave fronts and rays on the upper surface of a NACA 64A006 airfoil at M_∞ = 0.88 generated by an impulse source at the trailing edge: -----, wave front; ——, ray; ———, sonic line.

Figures 2 and 3 are constructed using the equations derived for the characteristic surfaces. The analysis assumed that ϕ and $\nabla\phi$ are continuous, and wave fronts are surfaces where the second-order derivatives of ϕ have jump discontinuities. Excluded from this assumption is the region where a shock wave exists and the ray equations are not applicable. However, the qualitative behavior of wave propagation can still be determined when the shock discontinuity is replaced by a continuous solution as follows,

$$C = 0, \qquad C_x \gg 1 \text{ on the shock} \tag{29}$$

For values of y where the shock wave is distinct, crowding of the wave fronts behind the shock is seen in Figs. 2 and 3. The waves in the subsonic region have normal vectors (p, q) pointing in the upstream direction so that $p < 0$. On approaching the shock, p decreases rapidly, resulting in a decrease in the phase velocity. Using Eq. (29), the Eikonal equation [Eq. (5)] defines a parabola, and the normal vector (p, q) can be shown to satisfy the following:

$$p \to -\infty, \qquad |q| \to +\infty, \qquad \frac{q}{p} \to 0 \tag{30}$$

This shows that the phase velocity c_{ph} will approach the horizontal direction and the phase speed $c_{ph} \to 0$. The wave fronts move slowly toward the shock and are normal to the airfoil surface.

Propagation Time

From the plot of rays in Fig. 2, it is evident that some of the rays originating from the trailing edge do not reach the shock wave. For different airfoil thicknesses and freestream Mach numbers, the maximum initial ray angle of a disturbance generated at the trailing edge that will reach the shock wave is determined. This critical ray angle α_{cr} is plotted vs the freestream Mach number in Fig. 4 where only cases having supercritical flowfields are considered.

For the three airfoils investigated, the thicker ones are found to have lower critical angles α_{cr} due to the larger supercritical flow regions, stronger shock waves, and the larger trailing-edge angles. The critical angle also decreases with increasing Mach number, up to a value of $M_\infty = 0.85$, above which it remains practically unchanged. An increase in M_∞ results in

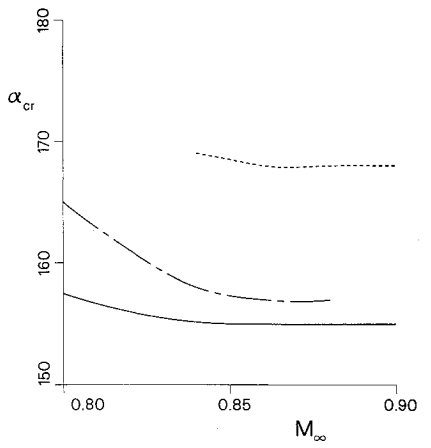

Fig. 4 Variation of critical angle α_{cr} with M_∞: —, NACA 0012; —·—, NACA 64A010; ----, NACA 64A006.

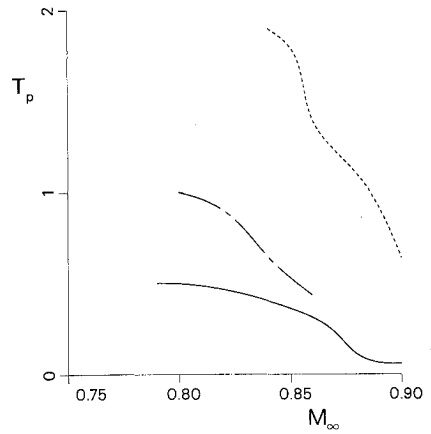

Fig. 5 Variation of propagation time T_p with M_∞: ——, NACA 0012; —·—, NACA 64A010; ----, NACA 64A006.

a lower value of α_{cr} because of the increase in shock strength. On the other hand, α_{cr} increases since the stronger shock will be located further downstream. These two effects tend to compensate each other and result in an approximately constant α_{cr} for $M_\infty > 0.85$. The minimum propagation time T_p, which is the time it takes a disturbance to travel from the source located at the trailing edge to the shock wave along the critical ray, is shown in normalized form with respect to c/U_∞, as a function of the freestream Mach number in Fig. 5. On increasing M_∞, the shock wave on the airfoil surface is stronger and is located closer to the trailing edge. This results in a lower propagation time, since the distance traveled by the disturbance to reach the shock wave is shorter. Increasing the airfoil thickness for constant M_∞ results in a stronger shock wave that forms farther aft toward the trailing edge. This will also result in a lower propagation time.

Tijdeman[1] proposed an approximate method for calculating the propagation time of Kutta waves emanating from the trailing edge. The time required for a disturbance to travel from the trailing edge to the shock wave is given as follows:

$$T = -\int_1^{x_s} \frac{dx}{(1 - M_{loc})a_{loc}} \tag{31}$$

where M_{loc} is the local Mach number, a_{loc} is the local velocity of sound, and the limits of integration are from the trailing edge ($x = 1$) to the shock wave x_s. The waves propagate along rays away from the airfoil surface. Hence, the propagation speed at any time is an intermediate value between the surface value of $(1 - M_{loc})a_{loc}$ and the freestream value. Tijdeman proposed the following approximation,

$$M_{loc} = R[M_{loc}(\text{at the surface}) - M_\infty] + M_\infty \tag{32}$$

where R is a relaxation factor between 0 and 1.

Tijdeman compared results using this approximation with experimental values obtained for an NLR 7301 airfoil at a freestream Mach number of 0.7, angle of attack of 3 deg, and unsteady pitch motion amplitude of 1 deg. In this comparison, it was found that a value of $R = 0.7$ produced good agreement. Using this value of R, the propagation time was computed for the cases considered in this study. Tijdeman intended the computation to be carried out on the surface of the airfoil. However, in this study, the integration of the approximate expression was carried out on a line starting at the trailing edge at a fixed initial angle. The angle α_I, which gives the best agreement between the propagation time obtained from Tijdeman's approximation and that from numerical integration of Eqs. (6), is shown as a function of the freestream Mach number in Fig. 6. It can be seen that α_I reaches an asymptotic value of approximately 170 deg for flowfields with strong shock waves, independent of airfoil thickness.

For weakly supercritical flowfields, α_I is less than 170 deg. The results for the 12 and 10% thick airfoils are closer together than the 6% airfoil, which does not have a region with supercritical flows at freestream Mach numbers less than 0.84. For $M_\infty < 0.875$, increasing the airfoil thickness increases α_I.

The sensitivity of the R value in Tijdeman's approximation in predicting the propagation time is shown in Fig. 7 for a 64A006 airfoil at a freestream Mach number of 0.85. For this case the shock wave location is at midchord. Three values—$R = 0.5$, 0.7, and 0.9—are used. Shown also in the figure is the time computed numerically using Eqs. (6). For $\alpha_I = 160$ deg, Tijdeman's approximation accurately computes the time using a value of $R = 0.7$. Increasing the value of R to 0.9

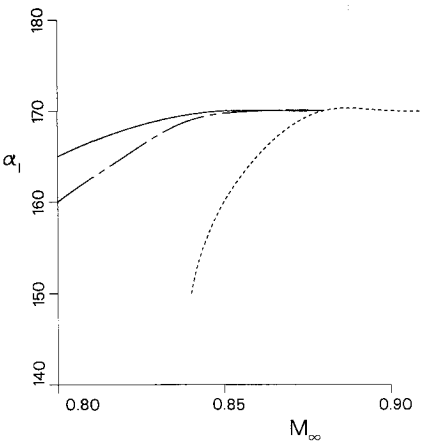

Fig. 6 Variation of α_I with M_∞: ——, NACA 0012; —·—, NACA 64A010; ----, NACA 64A006.

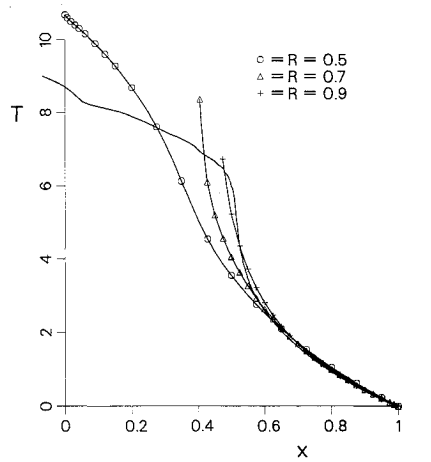

Fig. 7 Propagation time of wave fronts along $\alpha_I = 160$ deg at various values of R, for a NACA 64A006 airfoil at $M_\infty = 0.85$: ——, numerical.

increases T_p from 4 to 5, whereas a decrease of R to 0.5 gives $T_p = 3.5$. Also, a change of 5 deg in α_I produces a change of 0.17 in T_p. Varying the airfoil thickness gives different incremental changes in T_p for increasing values of R, but the trend is the same. These results indicate that Tijdeman's empirical formulation applied in the location between the shock wave and trailing edge is not very sensitive to R, and the value of 0.7 gives a good approximation of propagation time for the conventional airfoils investigated.

Impulse Source in a Time-Independent Medium

To illustrate the use of Eq. (28) in computing the amplitude of the disturbance, we give an example for the NACA 64A006 airfoil. The airfoil is stationary in a steady flow at $M_\infty = 0.85$ and at zero angle of attack. An impulse source is placed on the upper surface of the airfoil at the trailing edge $(x, y) = (1, 0)$. The source generates a disturbance of finite amplitude a_1 arbitrarily set at 100 units at time $t = 0$ and can be represented by a triplet $(x, y, a_1) = (1, 0, 100)$. At $t = t_1$, the disturbance propagates into the flowfield above the airfoil surface. If only the part of a wave front that is above the airfoil [$\alpha \in (104, 173$ deg)] is considered, it can be described by an arc in the (x, y) plane. The amplitude a_1 is zero everywhere in the flowfield except at the location of the wave front. In terms of the triplet, a curve is obtained in three-dimensional space (x, y, a_1), given parametrically by $[x(\alpha), y(\alpha), a_1(\alpha)]$.

Figure 8 shows the triples (x, y, a_1) on the upper surface of the airfoil. They are a family of curves for $t = 2.5, 5, 7.5, 10, 12.5$ deg, . . . , where the nondimensional t is given in degrees. At time $t = 2.5$ deg, the disturbance moves to a position indicated by the first curve closest to $(x, y) = (1, 0)$. Its amplitude decreases to approximately 50. At $t = 5$ deg, the disturbance is given by the second curve closest to $(x, y) = (1, 0)$. The amplitude is about 30–40. The 35th curve, for example, shows the disturbance at the time 87.5 deg. At this instance of time, part of the wave front has arrived at the shock that is located approximately at $(x, y) = (0.5, 0)$ on the airfoil surface. Because of the convergence of rays, the amplitude of the disturbances in the vicinity of the shock becomes much larger than the initial value of 100 units. In the limit, it approaches an infinite value when two rays coalesce. However, for presentation purposes, its amplitude is cut off at a value of 100 even though $a_1 > 100$ is detected at the shock wave.

Figure 9 is the projection of Fig. 8 onto the (x, y) plane. It shows the wave fronts generated by the impulse at different times. From the figure, crowding of wave fronts in the neighborhood of the shock wave can be observed.

Impulse Source in a Time-Dependent Medium

Figures 10–12 illustrate wave propagation in a time-dependent medium. The unsteady flow is generated from a NACA 64A006 airfoil with an oscillating flap motion. The Mach number is $M_\infty = 0.854$, and the reduced frequency $\kappa = 0.358$. The flap is located at $x = 0.75$ chord. The angle of oscillation is given by 1 deg $\sin(\omega t)$.

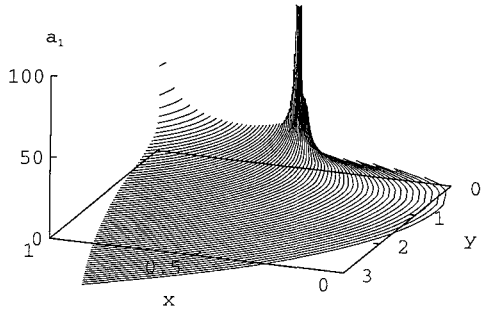

Fig. 8 Amplitude variation along wave fronts on the upper surface of a NACA 64A006 airfoil generated by an impulse source at the trailing edge at $M_\infty = 0.85$.

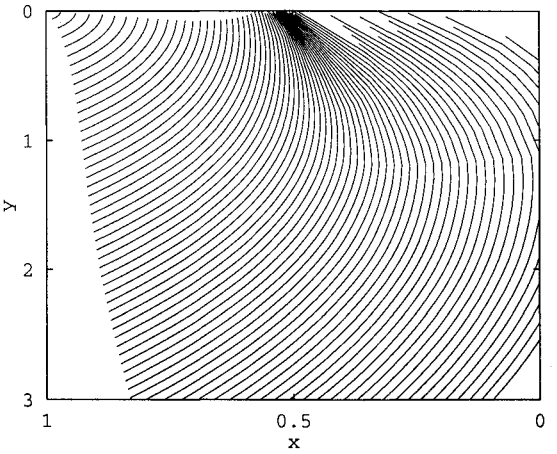

Fig. 9 Projection of wave fronts from Fig. 8 on the (x, y) plane.

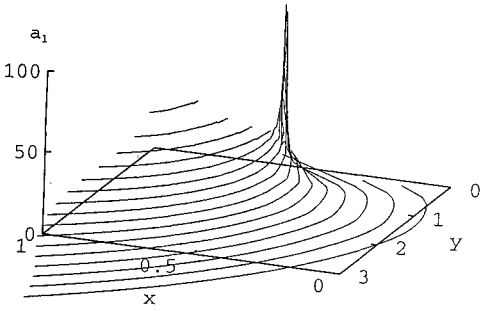

Fig. 10 Amplitude variation along wave fronts on the upper surface of a NACA 64A006 airfoil generated by an impulse source at the trailing edge of an oscillating flap: $M_\infty = 0.854$, $\kappa = 0.358$, and $t = 300$ deg.

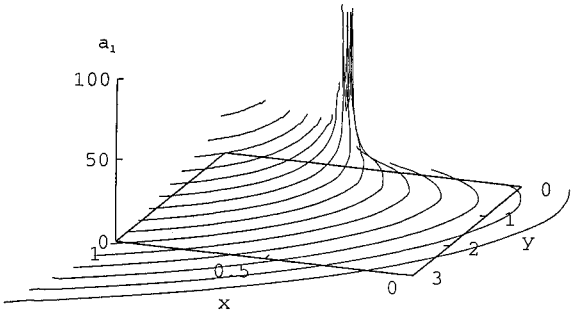

Fig. 11 Amplitude variation along wave fronts on the upper surface of a NACA 64A006 airfoil generated by an impulse source at the trailing edge of an oscillating flap: $M_\infty = 0.854$, $\kappa = 0.358$, and $t = 420$ deg.

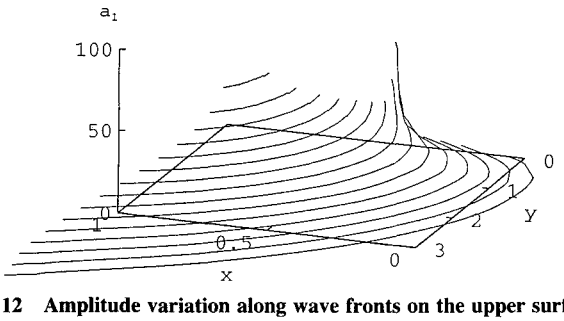

Fig. 12 Amplitude variation along wave fronts on the upper surface of a NACA 64A006 airfoil generated by an impulse source at the trailing edge of an oscillating flap: $M_\infty = 0.854$, $\kappa = 0.358$, and $t = 540$ deg.

A point source, located at (1, 0), generates impulses periodically, at time intervals of 12 deg. Since the flowfield is time dependent, two consecutive impulses will propagate in a different manner. If the first disturbance is generated at $t = 0$, then at $t > 0$, a total number of $t/12$ disturbances are present in the flowfield. Figure 10 shows the locations and amplitudes of disturbances at $t = 300$ deg for $\alpha \in (104, 173$ deg). At this time, a total of $25 = (300/12)$ impulses have been generated. Only those in the vicinity of the airfoil are shown here. Disturbances close to the shock have very large amplitudes. As in Fig. 8, a_1 is set to a maximum of 100 in this figure even though its value is greater than 100.

Figure 11 shows the disturbances at $t = 420$ deg. At this time, there are $35 = (420/12)$ wave fronts in the flowfield. Those that are omitted in the figures have propagated outside the region of interest near the airfoil. The supersonic region over the upper surface of the airfoil is larger than that at $t = 300$ deg, and the stronger shock wave results in larger amplitudes of the converging wave fronts.

Figure 12 shows the results for $t = 540$ deg. At this time, the supersonic region over the upper surface is small, and the shock wave is very weak. This results in smaller amplitudes in the neighborhood of the shock wave.

Conclusions

An analysis of the propagation of disturbances is carried out using the nonlinear transonic small disturbance equation. The method of characteristics is used to construct wave fronts generated by an impulse source located at an airfoil trailing edge.

The behavior of the disturbances depends on the flowfield around the airfoil. The presence of supersonic flow regions and shock waves has a pronounced effect on the wave propagation. The pressure change associated with the disturbances results in a perturbation to the shock position. The relation between the amplitude of the disturbance and the magnitude of shock displacement is currently under investigation. The results presented show the manner in which downstream disturbances interact with the shock wave and propagate into the supersonic flow region. This gives a better understanding of the feedback mechanisms proposed in an earlier investigation of oscillatory shock motion observed in transonic airfoil buffeting.

Tijdeman's empirical expression is used to evaluate the time it takes for disturbances generated at the trailing edge to reach the shock wave. The results compare favorably with the numerical computations when the angle of the line of integration in Tijdeman's expression is taken to be approximately 170 deg for a NACA 64A006 at freestream Mach numbers greater than 0.85. This angle is practically constant for conventional airfoil geometries, when $M_\infty > 0.875$. This investigation shows that Tijdeman's empirical formulation of the time for upstream wave propagation using a relaxation factor of 0.7 gives reasonable upstream propagation speeds for the conventional airfoils and Mach numbers considered.

The variation of the disturbance amplitude along the wave front can be determined using an asymptotic expansion method in the solution of the nonlinear wave equation. Wave propagation in both a steady and an unsteady medium has been investigated. For the latter case, disturbances generated at different times will propagate differently due to the time-varying flowfield. The more complicated case of the interaction of a harmonic disturbance with a shock wave having different frequencies of oscillation will be presented in a later paper. The analysis has aeroelastic applications, such as the study of wave propagation on an elastic wing performing oscillatory motion.

Acknowledgments

The authors gratefully acknowledge the financial support of the Institute for Aerospace Research, the Department of National Defence, and the Natural Sciences and Engineering Research Council of Canada.

References

[1]Tijdeman, H., "Investigation of the Transonic Flow Around Oscillating Airfoils," National Aerospace Lab., NLR TR-77090, Amsterdam, The Netherlands, Oct. 1977.

[2]McDevitt, J. B., "Supercritical Flow About a Thick Circular Arc Airfoil," NASA TM 78549, Jan. 1979.

[3]Mundell, A. R. G., and Mabey, D. G., "Pressure Fluctuations Caused by Transonic Shock/Boundary Layer Interaction," *Aeronautical Journal*, Vol. 90, Aug./Sept. 1986, pp. 274–281.

[4]Gibb, J., "The Cause and Cure of Periodic Flows at Transonic Speeds," *Proceedings of the 16th Congress of the International Council of Aeronautical Sciences* (Jerusalem, Israel), AIAA, Washington, D.C., Aug.–Sept. 1988, pp. 1522–1530.

[5]Stanewsky, E., and Basler, D., "Experimental Investigation of Buffet Onset and Penetration on a Supercritical Airfoil at Transonic Speeds," *Aircraft Dynamic Loads Due to Flow Separation*, AGARD-CP-483, Sept. 1990, pp. 4.1–4.11.

[6]Lee, B. H. K., "Oscillatory Shock Motion Caused by Transonic Shock Boundary-Layer Interaction," *AIAA Journal*, Vol. 28, No. 5, 1990, pp. 942–944.

[7]Lee, B. H. K., "Investigation of Flow Separation on a Supercritical Airfoil," *Journal of Aircraft*, Vol. 26, No. 11, 1989, pp. 1032–1037.

[8]Spee, B. M., "Wave Propagation in Transonic Flow Past Two-Dimensional Aerofoils," National Aerospace Lab., NLR-TN T. 123, Amsterdam, The Netherlands, July 1966.

[9]Whitham, G. B., *Linear and Nonlinear Waves*, Wiley, New York, 1974.

[10]Garabedian, P. R., *Partial Differential Equations*, Wiley, New York, 1964.

[11]Lee, B. H. K., Murty, H., and Jiang, H., "The Role of Kutta Waves on Oscillatory Shock Motion on an Airfoil Experiencing Heavy Buffeting," AIAA/ASME/ASCE/AHS/ASC 34th Structures, Structural Dynamics, and Materials Conference, AIAA Paper 93-1589, La Jolla, CA, April 1993.

[12]Couston, M., and Angelini, J. J., "Numerical Solutions of Nonsteady Two-Dimensional Transonic Flows," *Journal of Fluids Engineering*, Vol. 101, Sept. 1979, pp. 341–347.